Peristaltic Flow of a Carreau Fluid in a Channel with Different Wave Forms

T. Hayat,[1] **Najma Saleem,**[1] **N. Ali**[2]

[1] *Department of Mathematics, Quaid-i-Azam University 45320, Islamabad 44000, Pakistan*

[2] *Faculty of Applied Sciences, International Islamic University, Islamabad 44000, Pakistan*

Received 18 August 2008; accepted 17 November 2008
Published online 21 December 2009 in Wiley InterScience (www.interscience.wiley.com).
DOI 10.1002/num.20435

This investigation deals with the peristaltic motion of a Carreau fluid in a planar channel by employing long wavelength approximation. Five wave forms are chosen. Explicit solutions of longitudinal velocity and pressure gradient are derived. The pumping and trapping phenomena are properly examined. Comparison is made for the flow characteristics of the various selected wave forms. © 2009 Wiley Periodicals, Inc. Numer Methods Partial Differential Eq 26: 519–534, 2010

Keywords: Carreau fluid; pumping and trapping; symmetric channel

I. INTRODUCTION

It is known that the word peristaltic stems from the Greek word "peristaltikos," which means clapsing and compressing. The peristaltic flow can occur by the propagation of waves along the flexible walls of a channel/tube. Generally, it induces propulsive and mixing movements and pumps the fluid against pressure rise. In physiology, peristaltic motion is regarded as an inherent property of smooth muscle contraction. It is seen in the ureters, which are tubular organs connecting the kidneys to the bladder. It is an automatic process that moves food through the digestive tract, urine from the kidneys through the urteres into the bladder, bile from the gall bladder into the duodenum, spermatozoa in the ducts efferentes of the male reproductive tract, ovum in the female fallopian tube, lymph in the lymphatic vessel, and so on. Technical roller and finger pumps also operate according to the peristaltic action. Because of fluid diversity, many models have been proposed in the literature. Amongst the several fluid models, the simplest one is a Newtonian. Equations which can describe the flow of viscous fluid are the Navier-Stokes equations. There are many fluids whose flow behavior cannot be described by the Navier-Stokes equations. The inadequacy of the theory of Newtonian fluids in predicting the behavior of some fluids especially those of high molecular weight leads to the development of non-Newtonian fluid mechanics. The

Correspondence to: T. Hayat, Department of Mathematics, Quaid-i-Azam University 45320, Islamabad 44000, Pakistan (e-mail: pensy_t@yahoomail.com)
Contract grant sponsor: Higher Education Commission of Pakistan.

governing equations of non-Newtonian fluids are much more complicated and higher order than the Navier-Stokes equations. The solution of the involved equations of the non-Newtonian fluids offers interesting challenges to the investigators in the field. Even then various workers [1–24] are engaged in finding the solutions for flows involving Newtonian/non-Newtonian fluids.

Motivated by the aforementioned discussion, the object of this article is to investigate the peristaltic flow of Carreau fluid in a channel. The flow is induced by taking the peristaltic wave train on the channel walls. The chosen four-parameter Carreau fluid model has useful properties of a truncated power law model that does not have a discontinuous first derivative. It exhibits shear thinning properties. The flow features are seen in a wave frame of reference. The effects of various emerging parameters are studied on the pumping characteristics and trapping. The main findings of the presented analysis are summarized in the concluding remarks at the end.

Note that in Ref. [19], the authors have discussed the peristaltic motion of a Carreau fluid in an asymmetric channel. The problems are formulated in terms of stream function. This study is different from the analysis in Ref. [19] in two directions. Here, we consider the symmetric channel. In addition, different wave forms are taken into an account. The problem formulation here is made in terms of velocity components. Detail graphical analysis is presented and discussed.

II. GOVERNING EQUATIONS

Consider the peristaltic transport of an incompressible Carreau fluid in two-dimensional channel of width $2a$ .The flow is induced by periodic peristaltic wave of wavelength λ and amplitude b propagating with constant speed c along the channel walls. Its instantaneous height at any axial station X' is

$$Y' = H\left(\frac{X' - ct'}{\lambda}\right) \tag{1}$$

Five possible wave forms namely sinusoidal (s), multisinusoidal (ms), triangular (t), square (sq), trapezoidal (tr) waves are considered in this analysis.

In the laboratory frame (X', Y') the flow is unsteady. However, if observed in a coordinate system moving at speed c (wave frame), it can be treated as steady. The coordinates and the velocities in the two frames are related by

$$\begin{aligned} x' &= X' - ct', \quad y' = Y', \\ u'(x', y') &= U' - c, \quad v'(x', y') = V', \end{aligned} \tag{2}$$

where u' and v' indicate the velocity components in the wave frame.

The constitutive equations for Carreau fluid can be written as:

$$\bar{\tau} = -\left[\eta_\infty + (\eta_0 - \eta_\infty)(1 + (\Gamma\bar{\dot{\gamma}})^2)^{\frac{n-1}{2}}\right]\bar{\dot{\gamma}}, \tag{3}$$

$$\bar{\dot{\gamma}} = \sqrt{\frac{1}{2}\sum_i\sum_j \bar{\dot{\gamma}}_{ij}\bar{\dot{\gamma}}_{ji}} = \sqrt{\frac{1}{2}\pi}. \tag{4}$$

Here $\bar{\tau}$ denotes an extra stress tensor, η_∞ infinite shear stress viscosity, η_0 zero shear-rate viscosity, Γ the time constant, n the dimensionless power law index, and π the second invariant of strain-rate tensor.

Taking into account the case for which $\eta_\infty = 0$ one obtains the following equation

$$\bar{\tau} = -\left[\eta_0(1 + (\Gamma\bar{\dot{\gamma}})^2)^{\frac{n-1}{2}}\right]\bar{\dot{\gamma}}, \tag{5}$$

which reduces to viscous fluid situation for $n = 1$ or $\Gamma = 0$.

III. PROBLEM STATEMENT

The governing equations in the absense of body forces are

$$\nabla \cdot \bar{\mathbf{V}}' = 0, \tag{6}$$

$$\rho(\bar{\mathbf{V}}' \cdot \nabla)\bar{\mathbf{V}}' = -\bar{\nabla} p' + \mathrm{div}\bar{\tau}', \tag{7}$$

where $\bar{\mathbf{V}}'$ is the velocity vector, p' the fluid pressure, and $\bar{\boldsymbol{\tau}}'$ an extra stress tensor.The body forces are taken absent.

The definition of velocity is

$$\bar{\mathbf{V}}' = (u', v', 0). \tag{8}$$

We now write the nondimensional variables, the Reynolds number (Re) and wave number (δ) in the following manner:

$$x = \frac{x'}{\lambda},\ \ y = \frac{y'}{a},\ \ u = \frac{u'}{c},\ \ v = \frac{v'}{\delta c},\ \ t = \frac{t'c}{\lambda},\ \ h = \frac{H}{a},$$

$$\delta = \frac{a}{\lambda},\ \ Re = \frac{\rho c a}{\eta_0},\ \ p = \frac{a^2 p'}{c\lambda\eta_0},\ \ We = \frac{\Gamma c}{a},\ \ \Phi = \frac{a}{b},$$

$$\tau_{xx} = \frac{\lambda\tau'_{xx}}{\eta_0 c},\ \ \tau_{xy} = \frac{a\tau'_{xy}}{\eta_0 c},\ \ \tau_{yy} = \frac{a\tau'_{yy}}{\eta_0 c}. \tag{9}$$

Using above variables, Eqs. (6)–(8) give

$$\frac{\partial u}{\partial x} + \frac{\partial v}{\partial y} = 0, \tag{10}$$

$$Re\delta\left[u\frac{\partial}{\partial x} + v\frac{\partial}{\partial y}\right]u = -\frac{\partial p}{\partial x} - \delta^2\frac{\partial \tau_{xx}}{\partial x} - \frac{\partial \tau_{xy}}{\partial y}, \tag{11}$$

$$Re\delta^3\left[u\frac{\partial}{\partial x} + v\frac{\partial}{\partial y}\right]v = -\frac{\partial p}{\partial y} - \delta^3\frac{\partial \tau_{xy}}{\partial x} - \delta\frac{\partial \tau_{yy}}{\partial y}, \tag{12}$$

where

$$\tau_{xx} = -2\left[1 + \frac{(n-1)}{2}We^2\dot{\gamma}^2\right]\frac{\partial u}{\partial x}, \tag{13}$$

$$\tau_{xy} = -\left[1 + \frac{(n-1)}{2}We^2\dot{\gamma}^2\right]\left(\frac{\partial u}{\partial y} + \delta^2\frac{\partial v}{\partial x}\right), \tag{14}$$

$$\tau_{yy} = -2\delta\left[1 + \frac{(n-1)}{2}We^2\dot{\gamma}^2\right]\frac{\partial v}{\partial y} \tag{15}$$

in which We is the Weissenberg number.

Skukla et al. [25] and Srivastava and Srivastava [26] considered the long wavelength and low Reynolds number approximations for the mucus transport in small intestine. They showed that for small intestine $c = 2$ cm/min, $a = 1.25$ cm and $\lambda = 8.01$ cm. Therefore, under long wavelength and low Reynolds number approximations, Eqs. (11)–(15) give

$$\frac{\partial p}{\partial x} = \frac{\partial}{\partial y}\left[\left(1 + \frac{(n-1)}{2} We^2 \left(\frac{\partial u}{\partial y}\right)^2\right)\frac{\partial u}{\partial y}\right], \tag{16}$$

$$\frac{\partial p}{\partial y} = 0. \tag{17}$$

The above equation indicates that

$$p \neq p(y).$$

In the labortaory frame the dimensionless volume flow rate is defined by

$$Q = \int_0^H U(X', Y', t')dY', \tag{18}$$

where $H = H(X', t')$.

The above equation in the wave frame can be written as

$$q = \int_0^h u(x', y')\, dy', \tag{19}$$

in which $h = h(x')$.

Making use of Eqs. (2), (18), and (19) we obtain

$$Q = q + ch. \tag{20}$$

At fixed position X', the time-averaged flow over a period T is defined as

$$Q' = \frac{1}{T}\int_0^T Q dt \tag{21}$$

which after employing Eq. (20) becomes

$$Q' = q + ac. \tag{22}$$

If θ and F are the dimensionless mean flows in the laboratory and wave frames defined by

$$\theta = \frac{Q'}{ac}, \quad F = \frac{q}{ac} \tag{23}$$

then Eqs. (22) reduces to

$$\theta = F + 1, \tag{24}$$

$$F = \int_0^h u dy. \tag{25}$$

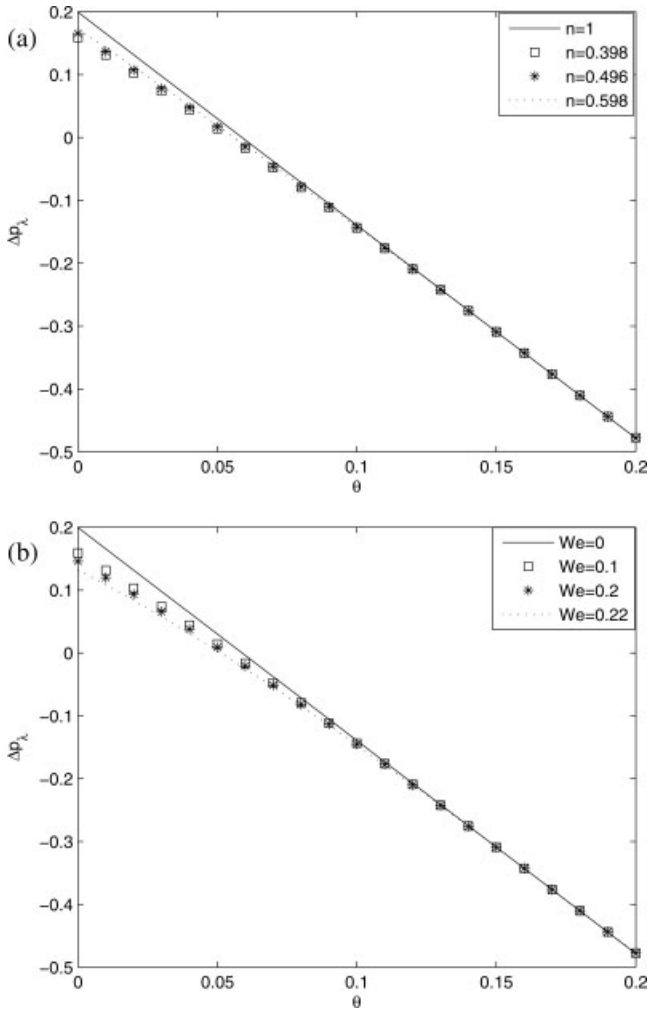

FIG. 1. (a) Plot showing Δp_λ versus flow rate θ for sinusoidal wave form. Here $\Phi = 0.2$, $We = 0.1$. (b) Plot showing Δp_λ versus flow rate θ for sinusoidal wave form. Here $\Phi = 0.2$, $n = 0.398$.

In the waveframe the boundary conditions of the problem are

$$\frac{\partial u}{\partial y} = 0 \quad \text{at } y = 0, \tag{26}$$

$$u = -1 \quad \text{at } y = h. \tag{27}$$

The expression of the pressure rise per wavelength (Δp_λ) is given by

$$\Delta p_\lambda = \int_0^1 \left(\frac{dp}{dx}\right) dx. \tag{28}$$

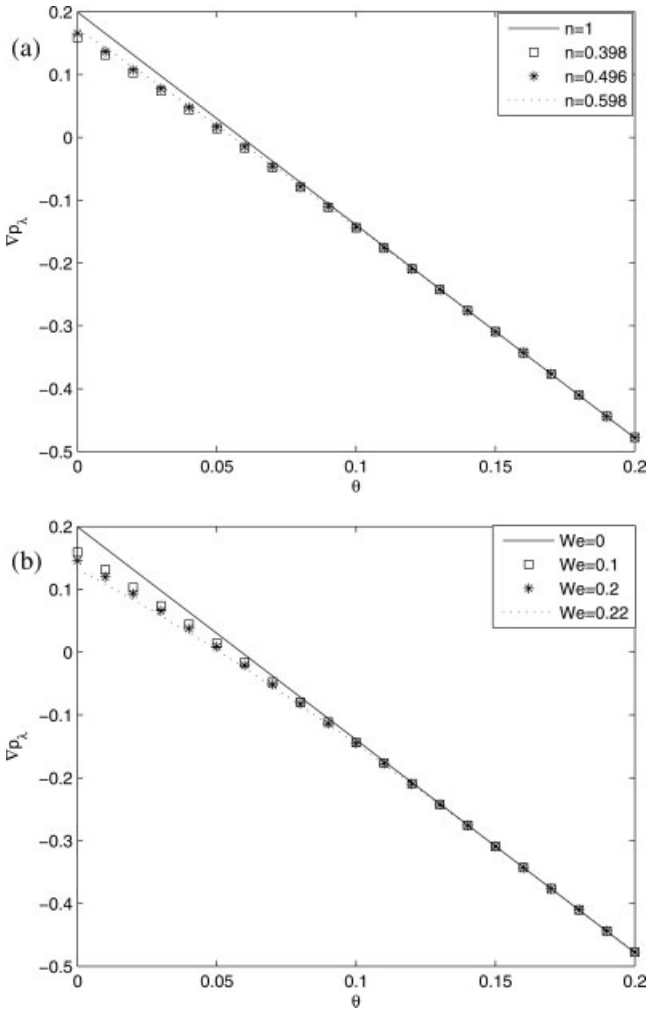

FIG. 2. (a) Plot showing Δp_λ versus flow rate θ for multisinusoidal wave form. Here $\Phi = 0.2$, $We = 0.1$, $N = 2$. (b) Plot showing Δp_λ versus flow rate θ for multisinusoidal wave form. Here $\Phi = 0.2$, $n = 0.398$, $N = 2$.

IV. PERTURBATION SOLUTION

In this section, our interest is to find the analytic solution of Eqs. (16), (26), and (27). The closed form solution of the arising problem is not easy to obtain. Therefore, we look for the perturbation solution. For such a solution, we write

$$u = u_0 + We^2 u_1 + O(We^4), \tag{29}$$

$$F = F_0 + We^2 F_1 + O(We^4), \tag{30}$$

$$p = p_0 + We^2 p_1 + O(We^4). \tag{31}$$

Substituting the above equations in Eqs. (16), (26), and (27) one has the following systems:

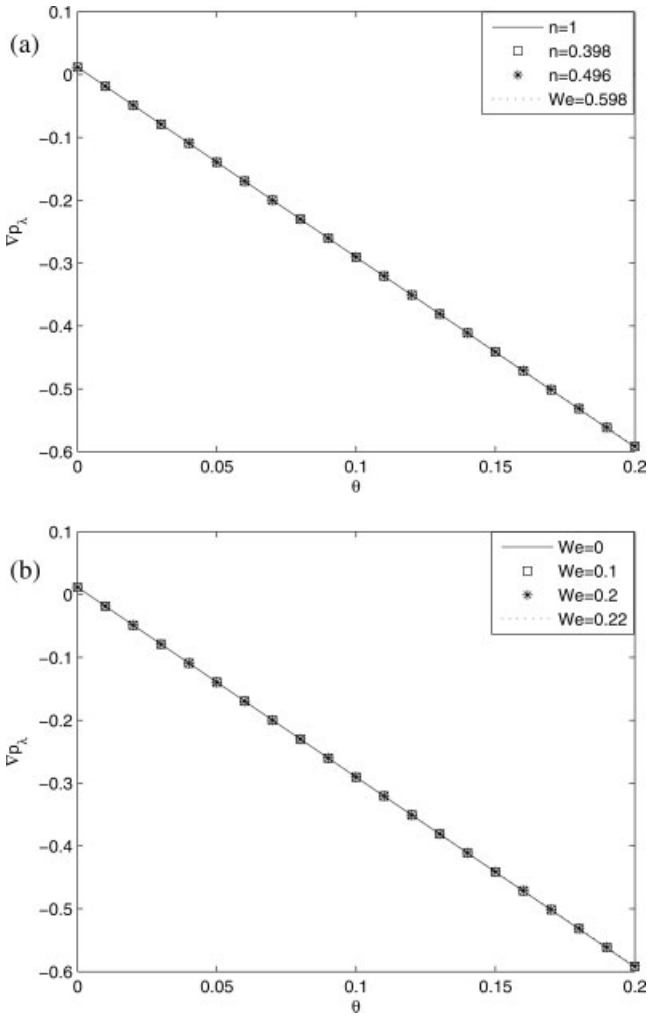

FIG. 3. (a) Plot showing Δp_λ versus flow rate θ for triangular wave form. Here $\Phi = 0.2$, $We = 0.1$. (b) Plot showing Δp_λ versus flow rate θ for triangular wave form. Here $\Phi = 0.2$, $n = 0.398$.

A. SYSTEM OF ORDER We^0

$$\frac{dp_0}{dx} = \frac{\partial^2 u_0}{\partial y^2}, \tag{32}$$

$$\frac{\partial u_0}{\partial y} = 0 \quad \text{at } y = 0, \tag{33}$$

$$u_0 = -1 \quad \text{at } y = h, \tag{34}$$

$$F_0 = \int_0^h u_0 dy, \tag{35}$$

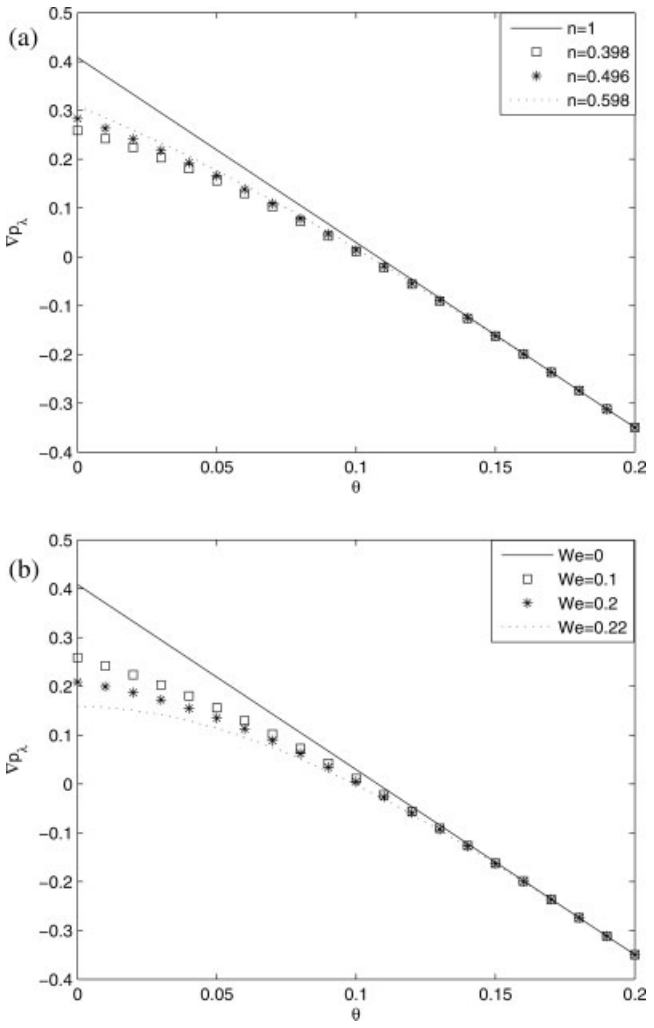

FIG. 4. (a) Plot showing Δp_λ versus flow rate θ for square wave form. Here $\Phi = 0.2$, $We = 0.1$. (b) Plot showing Δp_λ versus flow rate θ for square wave form. Here $\Phi = 0.2$, $n = 0.398$.

B. SYSTEM OF ORDER We^2

$$\frac{dp_1}{dx} = \frac{\partial^2 u_1}{\partial y^2} + \frac{(n-1)}{2}\frac{\partial}{\partial y}\left(\frac{\partial u_0}{\partial y}\right)^3, \tag{36}$$

$$\frac{\partial u_1}{\partial y} = 0 \quad \text{at } y = 0, \tag{37}$$

$$u_1 = 0 \quad \text{at } y = h, \tag{38}$$

$$F_1 = \int_0^h u_1 dy, \tag{39}$$

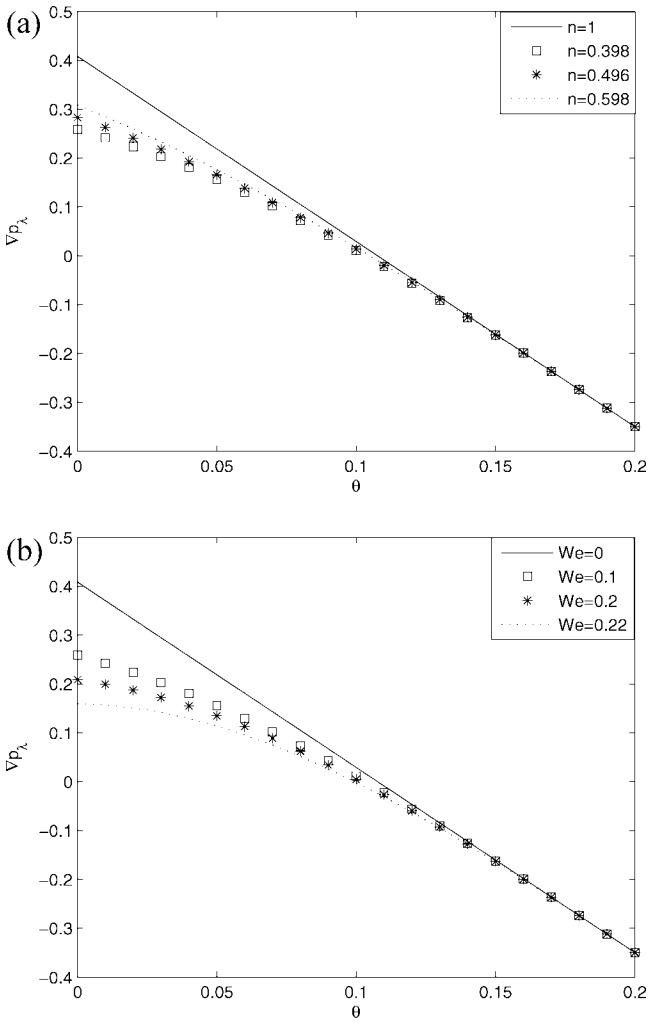

FIG. 5. (a) Plot showing Δp_λ versus flow rate θ for trapezoidal wave form. Here $\Phi = 0.2$, $We = 0.1$. (b) Plot showing Δp_λ versus flow rate θ for trapezoidal wave form. Here $\Phi = 0.2$, $n = 0.398$.

$$\Delta p_{\lambda_1} = \int_0^1 \frac{dp_1}{dx} dx. \tag{40}$$

C. SOLUTION OF SYSTEM OF ORDER We^0

The solution of Eqs. (32)–(34) is

$$u_0 = \frac{1}{2}\frac{dp_0}{dx}(y^2 - h^2) - 1. \tag{41}$$

$$\frac{dp_0}{dx} = -\frac{3}{h^3}(F_0 + h). \tag{42}$$

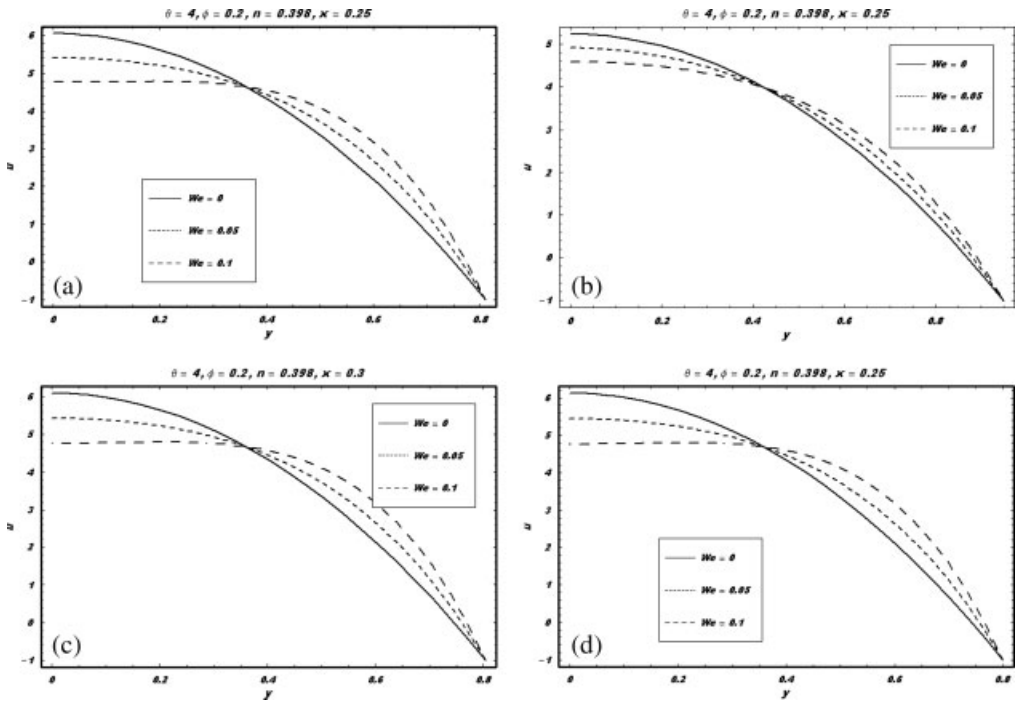

FIG. 6. (a) Plot showing velocity u versus y for narrow part of the channel for sinusoidal wave. (b) Plot showing velocity u versus y for narrow part of the channel for triangular wave. (c) Plot showing velocity u versus y for narrow part of the channel for square wave. (d) Plot showing velocity u versus y for narrow part of the channel for trapezoidal wave.

D. SOLUTION OF SYSTEM OF ORDER We^2

Here, the longitudinal velocity and pressure gradients are

$$u_1 = \frac{1}{2}\frac{dp_1}{dx}(y^2 - h^2) + \frac{(n-1)}{8}\left[\frac{3}{h^3}(F_0 + h)\right]^3 (y^4 - h^4). \tag{43}$$

and the expression of an axial pressure gradient at this order is

$$\frac{dp_1}{dx} = -\frac{3}{h^3}\left[F_1 + \frac{(n-1)\,h^5}{10}\left(\frac{3}{h^3}(F_0 + h)\right)^3\right]. \tag{44}$$

Expression of longitudinal velocity, axial pressure gradient, and pressure rise per wavelength upto $O(We^2)$ are

$$u = u_0 + We^2 u_1, \tag{45}$$

$$\frac{dp}{dx} = \frac{dp_0}{dx} + We^2\frac{dp_1}{dx}, \tag{46}$$

$$\Delta p_\lambda = \Delta p_{\lambda_0} + We^2 \Delta p_{\lambda_1}. \tag{47}$$

In the above solution, we use

$$F = F_0 + We^2 F_1 \tag{48}$$

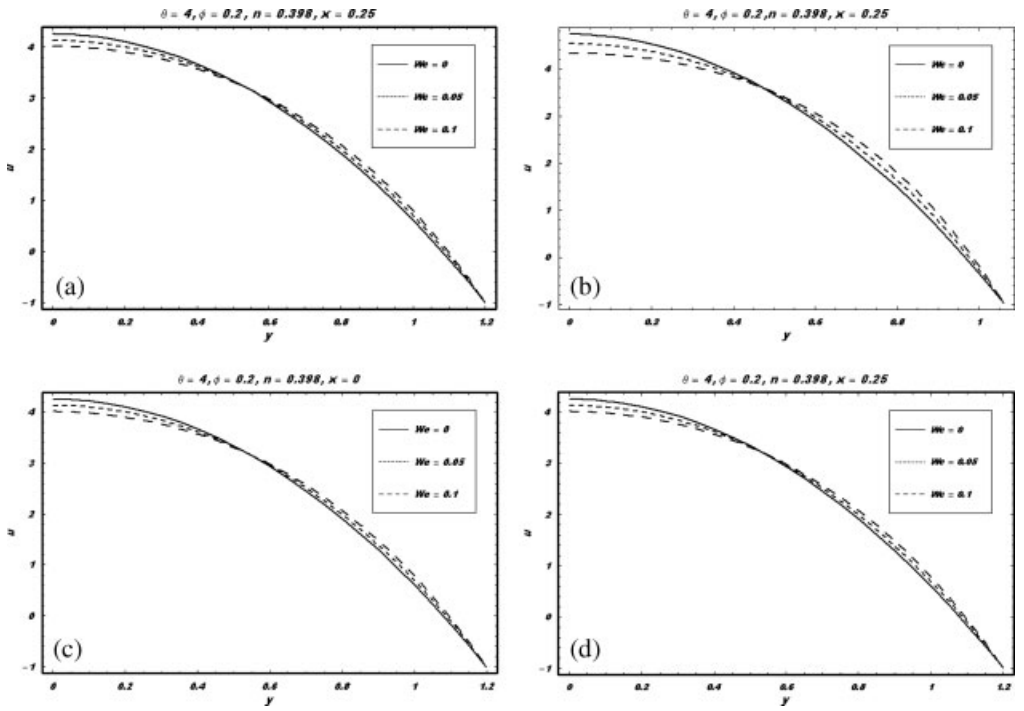

FIG. 7. (a) Plot showing velocity u versus y for wider part of the channel for sinusoidal wave. (b) Plot showing velocity u versus y for wider part of the channel for triangular wave. (c) Plot showing velocity u versus y for wider part of the channel for square wave. (d) Plot showing velocity u versus y for wider part of the channel for trapezoidal wave.

and neglect the terms that are greater than $O(We^2)$. The longitudinal velocity and pressure gradient after using Eq. (48) are

$$u = \frac{-3}{2h^3}(F+h)(y^2-h^2) - 1 + We^2\left[\begin{array}{c}(n-1)\left(\frac{3}{h^3}(F+h)\right)^3\\ \left(\frac{y^4-h^4}{8} - \frac{3h^2y^2-3h^4}{20}\right)\end{array}\right], \tag{49}$$

$$\frac{dp}{dx} = \frac{-3}{2h^3}(F+h) + We^2\left[\frac{-3h^2(n-1)}{10}\left(\frac{3}{h^3}(F+h)\right)^3\right]. \tag{50}$$

The stream function Ψ is

$$\Psi = \left[\frac{y}{2} + \frac{3(\theta-1)y}{2h} - \frac{(\theta-1)y^3}{2h^2} - \frac{y^3}{2h^2}\right] + We^2\left[\begin{array}{c} -\frac{27(\theta-1)^3y}{40h^5} - \frac{81(\theta-1)^2y}{40h^4} - \frac{81(\theta-1)y}{40h^3} - \frac{81y}{40h^2} + \frac{27(\theta-1)^2ny}{40h^5} + \frac{81(\theta-1)^2ny}{40h^4} + \frac{81(\theta-1)y}{40h^3}\\ +\frac{27ny}{40h^2} + \frac{27(\theta-1)^3y^3}{40h^7} + \frac{81(\theta-1)^2y^3}{20h^6} + \frac{81(\theta-1)y^3}{20h^5} + \frac{27y^3}{40h^4} - \frac{27(\theta-1)^3ny^3}{40h^7} - \frac{81(\theta-1)^2ny^3}{40h6} - \frac{81(\theta-1)ny^3}{20h^5}\\ -\frac{27ny^3}{20h^4} - \frac{27(\theta-1)^3y^5}{20h^9} - \frac{81(\theta-1)^2y^5}{40h^8} - \frac{81(\theta-1)y^5}{40h^7} - \frac{27y^5}{40h^6} + \frac{27(\theta-1)^3ny^5}{40h^9} + \frac{81(\theta-1)^2ny^5}{40h^8}\\ +\frac{81(\theta-1)ny^5}{40h^7} + \frac{27ny^5}{40h^6}\end{array}\right] - y. \tag{51}$$

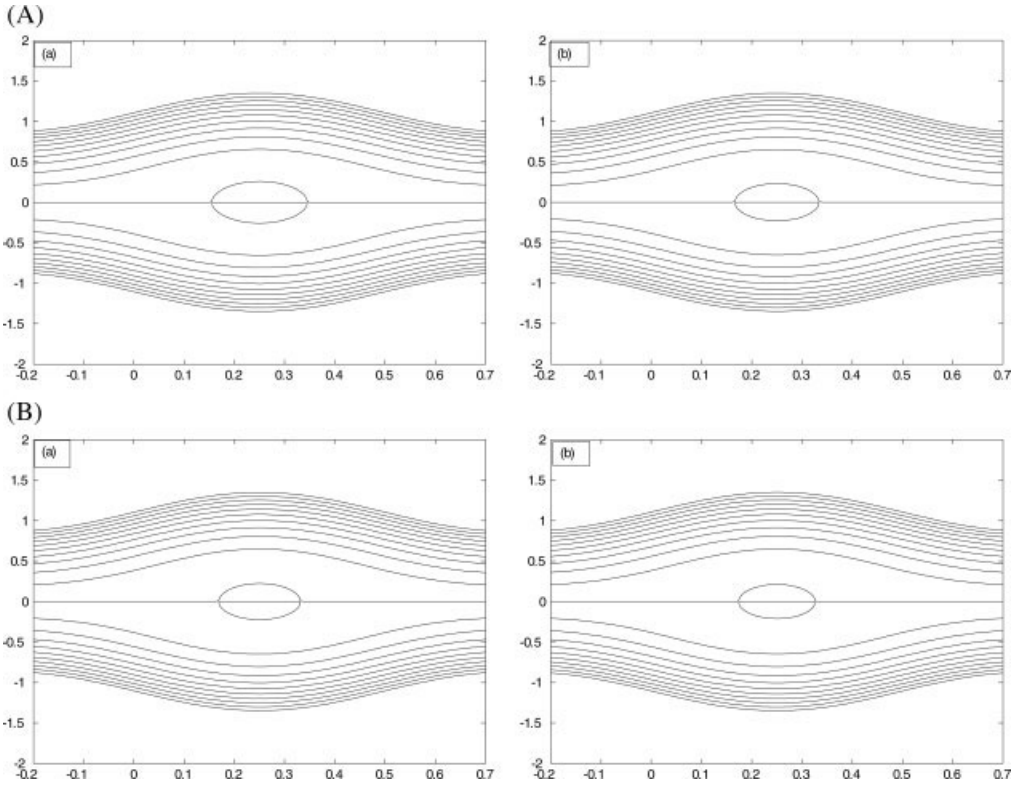

FIG. 8. (a) Streamlines for $n = 1$, (panel(a)), $n = 0.496$ (panel (b)). The other parameters are $\Phi = 0.2$, $We = 0.1$, and $\theta = 0.61$. (b) Streamlines for $We = 0.1$, (panel(a)), $We = 0.2$ (panel (b)). The other parameters are $\Phi = 0.2$, $n = 0.398$, and $\theta = 0.61$.

V. EXPRESSIONS FOR WAVE SHAPE

The nondimensional expressions of the considered wave forms are given by the following equations:

1. Sinusoidal wave

$$h(x) = 1 + \Phi \sin 2\pi x.$$

2. Multisinusoidal wave

$$h(x) = 1 + \Phi \sin 2N\pi x.$$

3. Triangular wave

$$h(x) = 1 + \Phi \left[\frac{8}{\pi^3} \sum_{m=1}^{\infty} \frac{(-1)^{m+1}}{(2m-1)^2} \sin\{2(2m-1)\pi x\} \right].$$

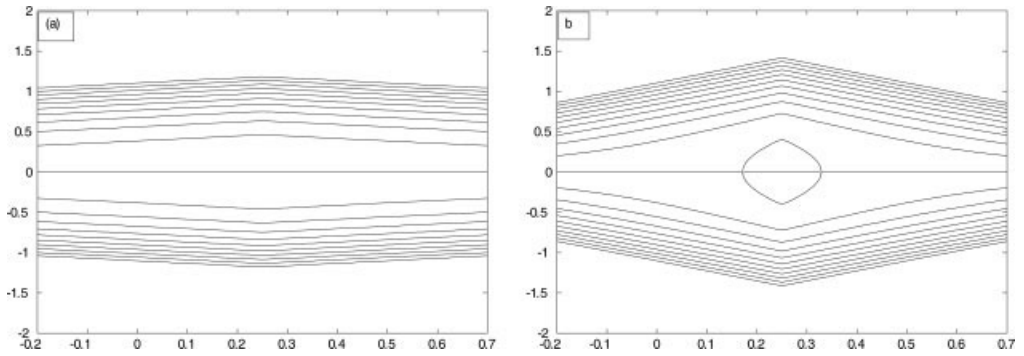

FIG. 9. Streamlines for $\Phi = 0.2$, (panel(a)), $\Phi = 0.8$ (panel (b)). The other parameters are $n = 0.398$, $We = 0.1$, and $\theta = 0.61$.

4. Square wave

$$h(x) = 1 + \Phi\left[\frac{4}{\pi}\sum_{m=1}^{\infty}\frac{(-1)^{m+1}}{(2m-1)}\cos\{2(2m-1)\,\pi x\}\right].$$

5. Trapezoidal wave

$$h(x) = 1 + \Phi\left[\frac{32}{\pi^2}\sum_{m=1}^{\infty}\frac{(-1)^{m+1}\sin\left\{\frac{\pi}{3}(2m-1)\right\}}{(2m-1)^2}\sin\{2(2m-1)\,\pi x\}\right].$$

Total number of terms in the series that are incorporated in the analysis are 50. Note that the expressions for triangular, square, and tapezoidal waves are derived from Fourier series.

VI. DISCUSSION

A. PUMPING CHARACTERISTICS

The expression for pressure rise per wavelength is evaluated numerically and is presented graphically for considered five wave forms. When pressure difference $\Delta p_\lambda = 0$, which is the case of free pumping, the corresponding time mean flow rate is denoted by θ_0. The maximum pressure against which the peristalsis works as a pump, that is, Δp_λ corresponding to $\theta = 0$ is denoted by p_0. When $\Delta p_\lambda < 0$, the pressure assists the flow and it is known as copumping. Figure 1(a,b) shows the variation of Δp_λ with flow rate θ for various values of dimensionless power law index n and Weissenberg number We, respectively, for sinusoidal wave form. We observe that $\theta_0|p_0$ decreases by increasing n and We. Further, in copumping, the pumping rate is independent of n and We. Similar results can be observed for multisinusoidal wave form (Fig. 2). It is interesting to note that when wave form is choosen to be triangular, the pumping rate is independent of values of n and We (Fig. 3). It is further noted from this figure that there is no peristaltic pumping for triangular wave. From Figs. 4 and 5, we observe that peristaltic pumping rate and free pumping flux decrease by increasing n and We, while in copumping the effects of n and We are negligible. Moreover, the pumping curves for square and trapezoidal wave have similar variation.

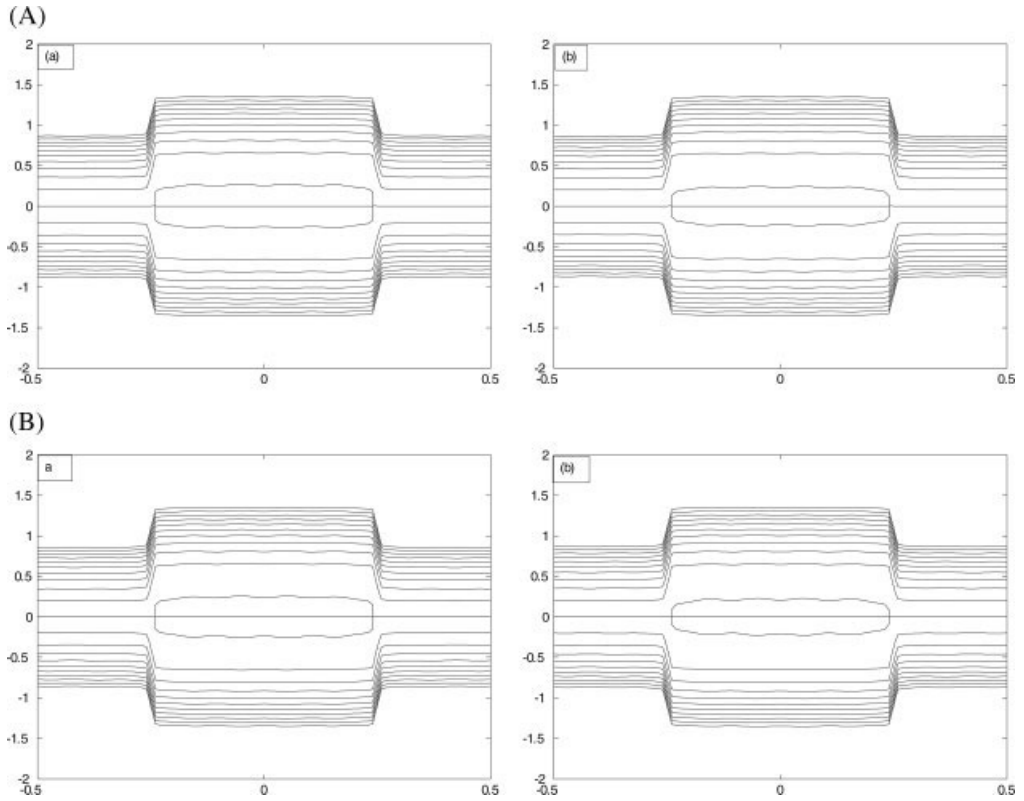

FIG. 10. (a) Streamlines for $n = 1$, (panel(a)), $n = 0.496$ (panel (b)). The other parameters are $\Phi = 0.2$, $We = 0.1$, and $\theta = 0.61$. (b) Streamlines for $We = 0$, (panel(a)), $We = 0.2$ (panel (b)). The other parameters are $\Phi = 0.2$, $\theta = 0.61$, and $n = 0.398$.

The longitudinal velocity $u(y)$ over two different cross-sections (narrow and wider parts) of the channel for different wave forms is presented in Figs. 6 and 7. It can be seen from these Figures that velocity decreases by increasing We near the center of the channel for all the considered wave forms. The magnitude of the velocity is less in the wider part of the channel when compared with the narrow part for all considered wave forms. In all these figures, the value of θ is equal to 4. For small values of θ, the effects of We on velocity are negligible.

B. TRAPPING

The formation of internally circulating bolus of fluid by closed streamlines is called trapping and this trapped bolus pushed ahead along with the peristaltic wave. The effects of n and We on trapping for different wave forms can be seen through Figs. 8–11. These figures show that by increasing (decreasing) We (n) the bolus squeez (i.e., its size reduces) for all the considered wave forms.

Intrestingly, for all the considered wave forms, trapping occurs at $\theta = 0.61$ and $\Phi = 0.2$. However, for triangular wave this is not the case. For triangular wave, the bolus appears only for large values of Φ or θ.

The authors thank the reviewers for their constructive comments.

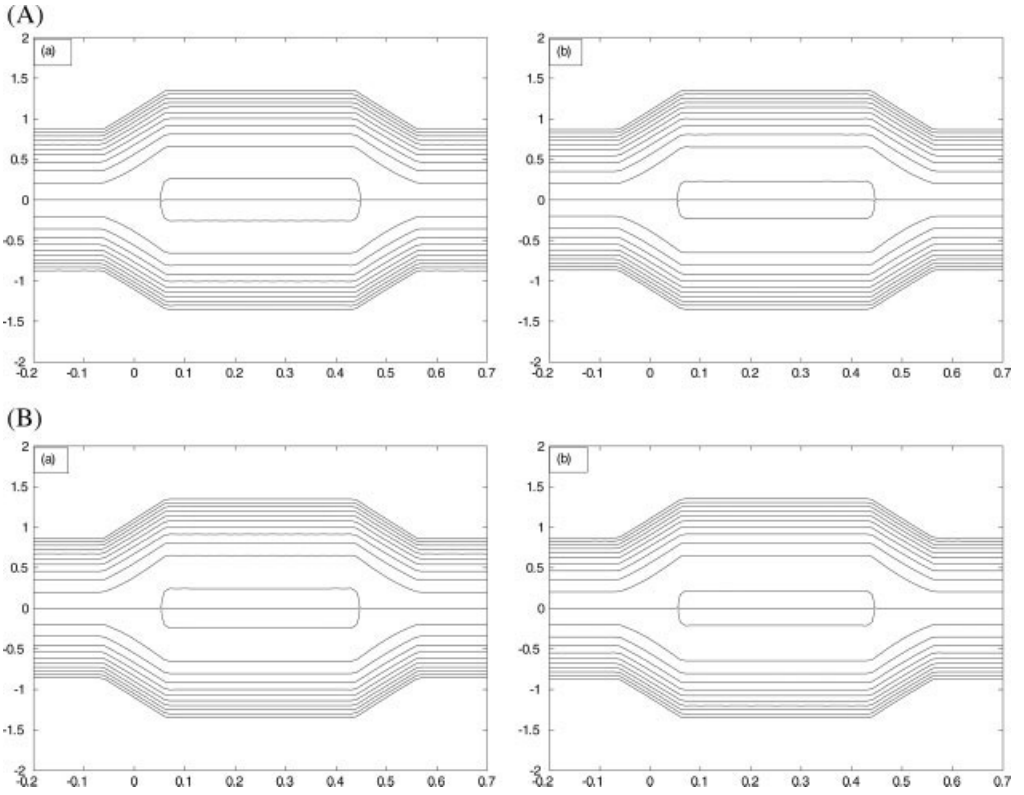

FIG. 11. (a) Streamlines for $n = 1$, (panel(a)), $n = 0.496$ (panel (b)). The other parameters are $\Phi = 0.2$, $We = 0.1$, and $\theta = 0.61$. (b) Streamlines for $We = 0$, (panel(a)), $We = 0.2$ (panel (b)). The other parameters are $\Phi = 0.2$, $\theta = 0.61$, and $n = 0.398$.

References

1. C. Fetecau and C. Fetecau, Unsteady motion of a Maxwell fluid due to longitudinal and torsional oscillations of an infinite circular cylinder, Proc Rom Acad Ser A 8 (2007), 77–84.
2. D. Vieru, C. Fetecau, and C. Fetecau, Flow of a viscoelastic fluid with fractional Maxwell model between two side walls perpendicular to a plate, Appl Math Comput 200 (2008), 459–464.
3. J. Zierep and C. Fetecau, Energetic balance for a Rayleigh-Stokes problem of a Maxwell fluid, Int J Eng Sci 45 (2007), 617–627.
4. C. Fetecau, C. Fetecau, and D. Vieru, On some helical flows of Oldroyd-B fluids, Acta Mech 189 (2007), 53–63.
5. M. Elshahed and M. H. Haroun, Rapid shear flows of dry granular masses down curved and twisted channels, Math Problems Eng 6 (2005), 663–677.
6. T. Hayat and K. Hutter, Rotating flow of a second order fluid on a porous plate, Int J Nonlinear Mech 39 (2004), 767–777.
7. T. Hayat, Y. Wang, and K. Hutter, Hall effects on the unsteady hydromagnetic oscillatory flow of a second grade fluid, Int J Nonlinear Mech 39 (2004), 1027–1037.
8. Y. Wang, T. Hayat, and K. Hutter, On non-linear magnetohydrodynamic problems of an Oldroyd 6-constant fluid, Int J Nonlinear Mech 40 (2005), 40–58.

9. W. C. Tan and T. Masuoka, Stokes' first problem for a second grade fluid in a porous half-space with heated boundary, Int J Nonlinear Mech 40 (2005), 515–522.

10. W. C. Tan and T. Masuoka, Stokes' first problem for an Oldroyd-B fluid in a porous half space, Phys Fluids 17 (2005), 0231011–0231017.

11. Kh. S. Mekheimer, Peristaltic transport of a couple stress fluid in uniform and non-uniform channels, Biorheology 39 (2002), 755–765.

12. Kh. S. Mekheimer, E. F. El Shehawey, and A. M. Alaw, Peristaltic motion of a particle-fluid suspension in a planar channel, Int J Theor Phys 37 (1998), 2895–2920.

13. E. F. El Shehawey and Kh. S. Mekheimer, Couple-stresses in peristaltic transport of fluids, J Phys D: Appl Phys 27 (1994), 1163–1170.

14. T. Hayat, Y. Wang, A. M. Siddiqui, and K. Hutter, Peristaltic motion of a Johnson-Segalman fluid in a planar channel, Math Problems Eng 1 (2003), 1–23.

15. T. Hayat, Y. Wang, A. M. Siddiqui, K. Hutter, and S. Asghar, Peristaltic transport of a third order fluid in a circular cylindrical tube, Math Models Methods Appl Sci 12 (2002), 1691–1706.

16. T. Hayat, Y. Wang, K. Hutter, S. Asghar, and A. M. Siddiqui, Peristaltic transport of an Oldroyd-B fluid in a planar channel, Math Problems Eng 4 (2004), 347–376.

17. A. M. Siddiqui, T. Hayat, and M. Khan, Magnetic fluid model induced by peristaltic waves, J Phys Soc Jpn 73 (2004), 2142–2147.

18. T. Hayat, F. M. Mahmood, and S. Asghar, Peristaltic flow of a magnetohydrodynamic Johnson-Segalman fluid, Nonlinear Dyn 40 (2005), 375–385.

19. N. Ali and T. Hayat, Peristaltic motion of a Carreau fluid in an asymmetric channel, Appl Math Comput 193 (2007), 535–552.

20. T. Hayat and N. Ali, On mechanism of peristaltic flows for power-law fluids, Physica A 371 (2006), 188–194.

21. T. Hayat and N. Ali, Peristaltically induced motion of a MHD third grade fluid in a deformable tube, Physica A 370 (2006), 225–239.

22. S. Srinivas and M. Kothandapani, Peristaltic transport in an asymmetric channel with heat transfer-A note, Int commun Heat Mass transfer 35 (2008), 514–522.

23. M. Kothandapani and S. Srinivas, Nonlinear peristaltic transport of a Newtonian fluid in an inclined asymmetric channel through a porous medium, Phys Lett A 372 (2008), 1265–1276.

24. S. Srinivas and M. Kothandapani, On influence of wall properties in the MHD peristaltic transport with heat transfer and porous medium, Phys Lett A 372 (2008), 4586–4591.

25. J. B. Shukla, R. S. Parihar, B. R. P. Rao, and S. P. Gupta, Effects of peripheral-layer viscosity on peristaltic transport of a bio-fluid, J Fluid Mech 97 (1980), 225–237.

26. L. M. Srivastava, V. P. Srivastava, and S. N. Sinah, Peristaltic transport of physiological fluid-2 flow in a uniform geometry, Biorheology 20 (1983), 153–166.